

**A LOW FORCE MELT VALVE FOR
DYNAMIC CONTROL OF MOLTEN PLASTICS**

SUBMITTED TO INTERNATIONAL POLYMER PROCESSING

**DAVID O. KAZMER & DHEERAJ GUPTA
DEPARTMENT OF PLASTICS ENGINEERING
UNIVERSITY OF MASSACHUSETTS LOWELL
LOWELL, MASSACHUSETTS 01854**

Contact: Dr. David O. Kazmer

Associate Professor, Department of Plastics Engineering

1 University Ave.

University of Massachusetts Lowell

Lowell, MA 01854, USA

Fax: 1-978-458-4141

E-mail: david_kazmer@uml.edu

ABSTRACT

Polymer processing has been limited by the lack of direct flow and pressure control of the polymer melt at multiple points in space and time. Improved axial and radial valve designs are discussed that require negligible actuation force to control the flow of the pressurized melt. The forces resulting from pressure loads and shear stresses are first analyzed for an axial valve pin. Subsequently, a radial valve design is implemented and experimentally characterized using neat polycarbonate. A sigmoidal response surface is fit to the experimental data and found to very well model the observed pressure drop as a function of flow rate and valve pin position. The juncture loss at the valve port is then characterized by estimating and removing the pressure drops in the circular flow segments of the valve. Analysis indicated that the juncture loss is inversely proportional to the exposed area, or vesica piscis, formed between the circular flow channel in the valve body and the flow port on the moving valve pin. While applicable to many different polymer processing operations, the validated models are used to show the dynamic valve pin position as a function of the desired flow rate and desired cavity pressure in the hot runner of an injection mold. Finally, the impact of the designs on lower power, more compact mechanical and control system designs are discussed.

KEYWORDS

Polymer processing; cavity pressure control; juncture loss; feed systems; valve design.

1. INTRODUCTION

Feed systems are used in polymer processing to deliver the polymer melt from the plastication unit to one or more molds or dies where the melt is formed. In many injection molds, for instance, multiple branches and gates are used in a feed system to deliver the melt to a plurality of locations so as to simultaneously form multiple articles in a single cycle, or alternatively to manufacture larger articles that could not be produced via a single gate. In conventional feed systems, including both cold and hot runners, the volumetric flow rate and pressure of the polymer melt is determined by the design of the feed system. Once specific lengths and diameters are machined, molding machines operating with conventional feed systems are not able to significantly change the dynamics of the polymer melt at one location without similarly affecting the polymer melt at other locations. As such, the different locations in a mold are coupled and the capability of molding processes is inherently limited, which often forces a compromise between multiple quality attributes. If process optimization does not lead to an acceptable compromise, then lengthy mold and/or material modifications are required. These changes, occurring late in the product development process, can incur significant cost and time penalties.

Earlier research led to a valve design, represented by the cross-section shown in Figure 1(a), for controlling the pressure at multiple points in an injection mold in real time [1-3]. This valve design controls the pressure drop and flow rate of the polymer melt with a tapered valve pin, wherein the valve pin position is moved axially to adjust the flow conductance and provide a corrective action in response to feedback from pressure transducers inside the mold cavity. This real time control allowed the flow rate at

multiple locations to be adjusted to, for example, move the weld line in the part, adjust the packing pressure in different areas of a mold, and perform other process feats. A limitation of this design, however, is that the forward movement of the valve pin to shut off the flow forces the positive displacement of polymer melt into the mold cavity, which results in a pressure surge and less precise control of the melt flow than desired.

Later research led to an improved valve design shown in Figure 1(b) that provides the valve sealing surface away from the gate, i.e. the moving valve pin retracts from the gate area to close [4-7]. This retraction of the valve pin results in a negative displacement of the melt from the gate, and an immediate reduction in the melt pressure in the mold cavity when closing. This behavior is desirable, since the closing of the valve is normally intended and required to correct an over-pressure situation. While the resulting design provides improved process flexibility and consistency, the performance of the system is limited by complexity, cost, size, shear degradation, energy consumption, and maintenance issues associated with the valve's design.

All these prior valve designs are subjected to the melt pressure, P_{melt} , acting on the entire projected area of the valve pin inside the feed system, and atmospheric pressure, P_{atm} , acting on the projected area of the valve pin outside the feed system. As a result, very high actuation forces, F , are required to control the location of the valve pin and flow through the valve:

$$F = \pi R^2 (P_{melt} - P_{atm}) \quad (1)$$

where R is the radius of the valve pin. For example, an injection molding process with a melt pressure of 100 MPa and a valve pin diameter of 8 mm would require an actuation force of 5,000 N. If a 5 mm stroke is required with a 10 mSec response time, then an

actuator with at least 2500 W of power would be required. This power requirement precludes the use of electric motors and pneumatic actuators, and in fact provides a practical limit to the number of hydraulic actuators that can be utilized in most molding applications.

DESIGN

If dynamic control of the polymer melt is to become common, it is necessary to design more compact valves that have improved dynamic response with lower actuation forces. Other important objectives include ease of use, ease of maintenance, and positive shut-off of the molten plastic at the gate as in a conventional valve gated hot runner system. Recognizing these objectives, a new valve design is presented based on two principles. First, the valve is designed such that the forces caused by the melt pressure are symmetric with respect to the axis of the valve pin. Second, the valve is designed such that all forces are symmetric with respect to the circumference of the valve pin. Accordingly, the actuation force required to move the pin is greatly reduced.

Two different valve designs are presented, including an axial valve shown in Figure 2 and a radial valve shown in Figure 3. While the valve designs are quite different, both designs rely upon juncture losses at the outlet of the valve pin's annulus rather than upon a pressure drop along the length of the valve pin as in the previous designs shown in Figure 1. The juncture loss results in a significant radial pressure gradient where the flow port in the valve pin restricts the flow at the valve body, though the symmetrical design of the valve pin precludes the development of axial forces. Specifically, the polymer melt in the axial valve shown in the Figure 2 will flow from the inlet and around the inlet

annulus. An annular flow port on the valve pin is adjusted via axial movement of the valve pin to constrict the flow to the outlet annulus, which then provides the flow to the outlet. The annuli are designed to provide negligible pressure drop compared to the juncture loss to minimize thrust loads on the valve pin. Also shown is an auxiliary primary opposite the inlet to provide melt flow to one or more downstream melt valves.

The radial valve design, shown in Figure 3, divides the melt flow into two flow segments to provide symmetric loadings to the valve pin rather than relying on an annulus with negligible pressure drop. The semicircular flows port on the valve pin are adjusted via radial movement of the valve pin to constrict the flow to the outlet flow segments, which then provide the flow to the outlet. There are two items to note regarding this design. First, the inlet and outlet flow ports are in-line with respect to the axis of the valve pin, which necessitates a level change inlet and outlet flow segments. Second, the radial valve can, in fact, be operated by moving the valve pin axially to constrict the flow at the flow ports.

The goal of the following analysis is to develop and predict the performance of an axial valve with minimal pressure drop, minimal shearing of the melt, minimal size, and fast response times. The primary design variables for a modified version of the axial valve are identified in Figure 4 and include the inlet/outlet diameter, $2R$, the outer diameter, aR , the inner diameter, bR , the extension diameter, cR , the annulus length, dR , and the valve pin position, eR .

The flow channels in the valve must be designed such that the minimum pressure drop when the valve is fully open is acceptable during operation. On the other hand, large flow channel diameters are undesirable due to the increase in the valve size and valve pin

inertia. Given a Newtonian fluid of viscosity, η , flowing at a rate, Q , through a pipe of length fR , the pressure drop is [8]:

$$\Delta P_{pipe} = \frac{8\eta f R Q}{\pi R^4} \quad (2)$$

There will also be a pressure drop through the annulus of the valve [8]:

$$\Delta P_{annulus} = \frac{8\eta d R Q}{\pi (aR)^4} \left[\left(1 - \left(\frac{b}{a}\right)^4\right) - \frac{\left(1 - \left(\frac{b}{a}\right)^2\right)^2}{\ln\left(\frac{a}{b}\right)} \right]^{-1} \quad (3)$$

For the design of the valve, allow the pressure drop to be equally distributed across the inlet, annulus, and outlet segments. Assuming for now that f , a , and d equal 2 with b/a equal to 0.5, then the nominal dimension, R , can be derived for a given viscosity, flow rate, and pressure drop. As an example, an application with a viscosity of 400 PaSec, a flow rate of 50 cc/sec, and an allowable pressure drop of 2 MPa (when fully open) would require a nominal dimension, R , of 4.8 mm.

Given the viscous flow of the polymer melt, there will be shear stresses which tend to pull the valve pin in the direction of flow, as well as a related pressure differential down the annulus that would tend to push the valve opposite the direction of flow. Since these forces counteract, it is desirable to design the valve pin such that the forces resulting from polymer flow through the valve are small during operation. Accordingly, the force on the valve pin due to the pressure drop along the length of the orifice is estimated as:

$$F_{\Delta P} = \Delta P_{annulus} \pi R^2 (a^2 - b^2) \quad (4)$$

where $\Delta P_{annulus}$ is provided by eq. 3. As the polymer melt flows along the valve pin, a shear stress, τ , will be exerted, which is approximately:

$$\tau = \frac{\Delta P_{annulus}}{2d} \left[b - \frac{(a^2 - b^2)}{2b \ln(a/b)} \right] \quad (5)$$

The resulting force on the valve pin due to this shear stress is estimated as:

$$F_{\tau} = \pi db R^2 \tau = \Delta P_{annulus} \pi R^2 \frac{b}{2} \left[b - \frac{(a^2 - b^2)}{2b \ln(a/b)} \right] \quad (6)$$

By comparing the forces due to the pressures and shear stresses acting on the valve pin, the valve pin may be designed to minimize the actuation force. Inspection of these equations indicates that the pressure forces predominate, so it is desirable to minimize the ratio of the inner to outer diameter, b/a , though this ratio is constrained by the allowable stress of the valve pin's material.

Continuing with the previous example, Figure 5 shows the estimated forces acting on a valve pin as a function on inner to outer diameter, b/a . It is observed that the forces due to the pressure differential across the valve increase more quickly with b/a than the forces due to the shear stress on the valve pin. In particular, it is observed that the forces increase precipitously for values b/a greater than 0.5, so this value is selected. The net resultant force on the valve is approximately 30 N, less than 0.5% of the 7500 N required to actuate prior valve designs of similar size.

EXPERIMENTAL

It is desirable for controllability purposes that the valve design provides a broad range of positions across which the flow rates are continuously adjustable. Experimental and analytical investigations with the prior valve designs have indicated that the flow rate through the valve is a highly non-linear function of the valve position. When the valve is closed, there is no flow through the valve. As the valve opens slightly, the gap between

the valve pin and the valve body is very small (ref. Figure 1) such that very little flow is transmitted. As the valve opens further, the flow conductance increases substantially such that the flow rate is no longer constrained by the valve, but rather by the flow conductance of the entire feed system including the upstream and downstream segments. As such, the flow rate behavior in the previous designs appears to be a sigmoidal function with asymptotes at the valve's closed and open positions. While this function is highly non-linear, the flow behavior through the previously designed valves was sufficient for maintaining flow control.

The new designs, however, rely upon a different phenomenon for controlling flow as a function of valve pin position. As such, a primary concern is that these new valve designs (that utilize a juncture loss) may provide too sharp a transition from no flow to full flow, such that dynamic control is not enabled with resolvable changes in the valve pin position. To characterize the new valves' ability to control flow, the radial design shown in Figure 3 was constructed with pressure transducers installed at the inlet and the outlet of the valve.* The assembled system was installed as a replacement nozzle on an 80 ton HPM tiebarless molding machine. This machine has a 9:1 intensification ratio between the melt pressure and the hydraulic pressure. The material was a low viscosity PC, Lexan SP1010 (GE Plastics) processed with a melt temperature of 288C.

A 24 run full factorial design of experiments, shown in Table 1, was utilized to fully characterize the valve's behavior at eight different valve positions and three different inlet melt pressure levels. According to previous experience, the eight valve positions

* A modified design of the axial design has also been validated for use as an open loop melt pressure regulator, and is the subject of a companion paper.

were selected with bias towards the closed (or zero) position. The three pressures were selected to provide adequate melt pressure to drive the flow while investigating possible curvature of the pressure dependence.

The results are provided in Table 1, where P_{hyd} is the hydraulic pressure supplied to the injection cylinder, P_{in} is the pressure measured at the inlet, P_{out} is the pressure measured at the outlet, ΔP is the pressure drop across the valve, and Q is the measured flow rate. It is observed from the data that the flow rate is strongly dependent on both the pressure and the valve pin position. To better understand the flow behavior, the data was fit to a modified sigmoidal function:

$$Q(x, P) = \left(\frac{a \cdot e^{c \cdot x} - a \cdot e^{-c \cdot x}}{e^{c \cdot x} + b \cdot e^{-c \cdot x}} \cdot \Delta P \right)^d \quad (7)$$

where x is the valve pin position from 0 to 100%, a controls the nominal flow rate through the valve, b controls the skewness of the flow rate dependence, c controls the sharpness of the rise in flow rate with increasing x , and d is related to the power law index of the melt. The coefficients were determined by a minimization of the sum of squared error defined as:

$$SSE = \sum_{i=1}^{24} (Q_i - \hat{Q}_i)^2 \quad (8)$$

where Q_i is the observed flow rate at the i -th run, and \hat{Q}_i is the predicted flow rate for the i -th run given the observed pressure drop and the set valve position. While the sigmoidal function is non-linear, an R^2 value can be evaluated by comparing the sum of squared error to the sum of the observed variance, SV :

$$R^2 = \frac{SSE}{SV} = \frac{SSE}{\sum_{i=1}^{24} (Q_i - \bar{Q})^2} \quad (9)$$

where \bar{Q} is the observed average flow rate. Accordingly, the R^2 value is commonly used to determine the proportion of behavioral variation that is described by the response surface. The model coefficients are provided in Table 2 together with the fitting statistics. The fit is quite remarkable, since the model with only four coefficients explains 98.9% of the observed behavior across twenty four observations leaving twenty degrees of freedom. As such, the resulting response surface is assumed a valid representation of the valve's flow rate behavior for given pressure drops and valve pin positions.

Figure 6 shows the flow rate as a function of valve pin position for several different pressure drops. As can be observed, the flow rate increases monotonically from a zero asymptote in the closed position to a second asymptote when the flow port in the valve pin is in a fully open position. Somewhat surprisingly, the rise of the flow rate is quite gradual. Compared to the flow rate behavior of the previous valve designs, the observed flow rate indicates that the new valve design should be quite capable of dynamically controlling flow by adjusting the pin position.

Figure 7 shows the flow rate as a function of pressure drop for several different valve pin positions. As can be observed, the flow rate increases with the supplied pressure drop. The curvature is attributable to the shear thinning of the polymer melt, which reduces the melt viscosity at higher flow rates. Given a typical flow rate of 100 cc/sec in injection molding, the results indicate a pressure drop of less than 10 MPa across the valve. If this pressure drop is unacceptable, or if significantly higher flow rates are desired, then it is possible to select a larger nominal dimension, R , according to the foregoing analysis.

ANALYSIS

To understand the juncture loss as a function of pin position, it is necessary to remove the pressure drop through the other flow channels of the low force valve from the total observed pressure drop. The low force valve may be decomposed into a series of passageways, and modeled using an equivalent circuit analogy as shown in Figure 8. In this representation, the flow resistance of each segment can be computed using the well established relationship between flow rate and pressure [9]:

$$\Delta P = \left(\frac{Q(s+3)}{\pi R^3} \right)^n \frac{2mL}{KR} \quad (10)$$

assuming a power-law model that provides a straight line relation between the log of the viscosity and the log of shear rate:

$$\eta(\dot{\gamma}) = m\dot{\gamma}^{n-1} \quad (11)$$

where m is the reference viscosity at a shear rate of 1/sec, n is the power law index, and s is the reciprocal of n . In eq. 10, the coefficient K is a shape factor coefficient of 1.0 for circular segments and 0.447 for the semi-circular geometry used in the ports of the valve pin [10]. Given a nominal diameter of 8 mm in all flow segments, the shear rates at the experimental conditions have been calculated and found to range from 0 to 10,000 1/sec. A power-law model was fit to rheology data at these shear rate conditions resulting in m and n of 629 and 0.76, respectively.

Using the derived response surface of eq. 7, the pressure drop through the low force valve was calculated at flow rates of 10 cc/sec, 20 cc/sec, 40 cc/sec, and 80 cc/sec. Higher flow rates were not evaluated since these conditions exceeded the experimental

observations and would result in potentially invalid extrapolations of the response surface and rheological data. According to eq. 10, the pressure drop through all the flow segments was removed from the total pressure drop through the low force valve to provide an estimate of the juncture loss at various flow rates. The juncture loss is plotted on a log scale as a function of valve pin position in Figure 9.

There are several conclusions that can be drawn from Figure 9. First, the set of curves on the log plot correspond to an exponential series of flow rates and have equal spacing, which indicates that the juncture loss has a power law relation with the flow rate, at least in this flow rate regime with shear rates less than 10,000 reciprocal seconds. Second, the juncture loss is highly non-linear with respect to the pin position. Starting from the right of the plot, there appears to be a broad plateau when the valve pin is mostly open and there are very small pressure drops. There then appears to be a log-linear relationship for valve openings between 50% and 5% open. Finally, there appears to be an asymptote for very small valve openings where the juncture loss approaches infinity.

For the radial valve design, the two intersecting circles corresponding to the flow segments in the valve body and the flow ports in the valve pin form a “vesica piscis” [11]. The overlapping, or exposed, area as a function of pin position, d , is [12]:

$$A = 2R^2 \cos^{-1}\left(\frac{d}{2R}\right) - \frac{1}{2}\sqrt{(2R-d)(2R+d)d^2} \quad (12)$$

A review of flow conductance equations (e.g. eq. 10) suggests that the juncture loss might be proportional to the exposed area and the power law index, n , according to the relation:

$$\Delta P_{juncture} \propto \left(\frac{Q}{A}\right)^n \quad (13)$$

The validity of this relationship is confirmed in Figure 10. Specifically, the results indicate that for n equal to 0.76, the pressure drop through the juncture is inversely proportional to the exposed area raised to the power law index. While not shown in Figure 10, linear regression was performed on each of the curves indicated all R^2 values exceeded 0.99 for all flow rates investigated.

DISCUSSION

The foregoing research sought to characterize the behavior of the radial valve, and develop fundamental models that govern the design performance. Based on these models, it is possible to predict the pin position for a typical injection molding cycle utilizing the radial valve to dynamically control the melt flow and pressure to a downstream cavity. Figure 11(a) shows a desired flow rate profile as a function of time at a downstream cavity. Figure 11(b) shows the injection pressure profile at the nozzle of the molding machine, the desired downstream cavity pressure, and the calculated pressure drop from the machine nozzle through the low force valve to the cavity. According to the described models, Figure 11(c) provides the calculated pin position required to simultaneously satisfy the specified flow rate and pressure drop through the valve. It is observed that the valve pin position will vary continually during the filling and packing stages of the molding process. Given that higher flow rates are required during filling, the valve pin will be in a mostly open position. With lower flow rate and/or higher pressure drop requirements, the valve pin will move to a mostly closed position.

Given that the feasibility of the valve design is established, some discussion is warranted regarding its potential impact. By providing lower actuation forces, the new

designs allow improved performance and lower costs. Specifically, the lower actuation forces allows for smaller and lower power actuators, such as the replacement of hydraulic actuators with pneumatic actuators or electric motors. Alternatively, the valve pins and orifices can be made larger to allow for higher volumetric flow rates with lower shear rates than would otherwise be possible. As a third alternative, the response time of the valve pin can be greatly improved compared to prior designs with the same power consumption.

With respect to implementation in hot runner systems for injection molding, the axial valve pin design may be augmented with a valve pin extension that contacts the downstream melt flow near the gate of the injection mold. Such a design is shown in Figure 12 and can be used to provide positive shut-off of the flow just as a conventional valve gate. In this design, the actuation force will be driven primarily by the diameter of the valve pin at the gate and the local pressure at the gate. Fortunately, the diameter of the valve pin at the gate may be much smaller than the diameter of the metering section of the valve pin, such that the required actuation forces are on the same order as those for a conventional valve gate. Furthermore, since the actuation forces will now be largely proportional to cavity pressure, the load on the valve pin may be ascertained with a strain gage to provide a reasonable estimate of cavity pressure without the need for a separate pressure transducer. Such a valve design thereby enables improved cavity pressure control with reduced instrumentation cost, reduced actuator size and cost, and reduced energy cost than the previous designs.

With respect to the valve pin actuator itself, the valve pin can be moved via electric, pneumatic, or hydraulic power with cylinders, screws, gears, and other power

transmission elements. It is desirable to rapidly actuate the valve pin, and also hold the pin position without consuming much power. The use of an electric actuator provides several advantages which could facilitate adoption of the new valve designs by the industry. First, the electric motor avoids the use of fragile, bulky, and costly pneumatic or hydraulic hoses. Second, the electric motor provides very fast initial response. Third, the electric motor provides a method for estimating the load on the valve pin and thereby estimating the melt pressure by monitoring current consumption. Fourth, the electric motor provides a method for estimating the position of the valve pin by monitoring motor command signals. Given the lower operating temperature and power density of electric motors compared to similarly sized hydraulic systems, the development of an all-electric system requires a precise understanding of the power consumed in actuating the low force valve, and is the subject of on-going research.

CONCLUSIONS

The paper presented axial and radial valve designs that require greatly reduced actuation forces compared to previous designs. The characterization of the radial valve indicated that these designs based on the juncture loss between the flow inlet and flow port provide the flow control required.

Dynamic control of the polymer melt in space and time provides enormous benefits in polymer processing, though cost and complexity issues related to instrumentations and actuation must be addressed prior to widespread adoption. Towards this end, a self-regulating valve has been developed from the axial design, in which the load from the melt pressure counteracts a control force to provide a regulated outlet pressure via an open loop control architecture without any pressure transducers. Another thrust of on-

going research is the on-line fusion of sensor data with faster than real time simulation to provide estimates of the flow rate, viscosity, and other part quality attributes every two milliseconds. Finally, research is quantifying the extent of mechanical and thermal degradation of polymer melts passing at high rates through small junctures.

ACKNOWLEDGEMENTS

Portions of this work were funded by National Science Foundation Grant No. 02-045309. The contents of this paper do not represent the opinions of the National Science Foundation or the United States Government.

BIBLIOGRAPHY

- [1] D. O. Kazmer, "Introduction to dynamic feed control for injection molding," presented at Proceedings of the 52nd Annual Technical Conference ANTEC, Part 1 (of 3), 1994.
- [2] D. O. Kazmer and P. Barkan, "Multi-Cavity Pressure Control in the Filling and Packing Stages of the Injection Molding Process," *Polymer Engineering and Science*, vol. 37, pp. 1865-1879, 1997.
- [3] D. O. Kazmer and P. Barkan, "The Process Capability of Multi-Cavity Pressure Control of the Injection Molding Process," *Polymer Engineering and Science*, vol. 37, pp. 1880-1897, 1997.
- [4] D. Kapoor and D. Kazmer, "Consistency of multi cavity melt control injection molding in a commercial application," presented at Proceedings of the 56th Annual Technical Conference, ANTEC, Part 1 (of 3), 1998.
- [5] D. Kapoor and D. Kazmer, "Consistency and Flexibility of Multi Cavity Melt Control Injection Molding in a Commercial Application," *International Polymer Processing*, vol. 13, pp. 398-405, 1998.
- [6] B. Cahill, M. Doyle, D. Kazmer, M. Moss, and M. Niemeyer, "Utilization of dynamic feed control for commercial applications," presented at Proceedings of the 56th Annual Technical Conference, ANTEC, Part 1 (of 3), 1998.
- [7] J. Reilly, M. Doyle, and D. Kazmer, "An Assessment of Dynamic Feed in Modular Tooling," presented at Annual Technical Conference, Dallas, TX, 2001.
- [8] Z. Tadmor and C. G. Gogos, *Principles of Polymer Processing*: John Wiley & Sons, 1979.

- [9] J. Agassant, P. Avanas, J. Sergent, and J. Garreau, *Polymer Processing: Principles and Modeling*, 1991.
- [10] G. Menges, W. Michaeli, and P. Mohren, "How to Make Injection Molds," 3rd ed: Hanser, 2001.
- [11] M. S. Schneider, *A Beginner's Guide to Constructing the Universe*: Harper Collins, 1994.
- [12] E. W. Weisstein, *CRC Concise Encyclopedia of Mathematics*, 2nd ed: CRC Press, 2002.

Table 1: Experimental Run Conditions and Results

<i>Run</i>	<i>Valve Position</i>	P_{hyd} (MPa)	P_{in} (MPa)	P_{out} (MPa)	ΔP (MPa)	Q (cc/s)
1	100%	0.7	6.1	1.3	4.8	34.9
2		2.1	15.0	2.4	12.6	108.6
3		3.4	22.7	3.1	19.6	197.1
4	50%	0.7	6.0	1.2	4.8	26.6
5		2.1	14.9	2.3	12.6	94.7
6		3.4	23.3	3.0	20.3	169.5
7	30%	0.7	6.3	1.1	5.2	26.6
8		2.1	16.2	2.1	14.1	72.4
9		3.4	24.1	2.7	21.3	139.8
10	20%	0.7	6.6	0.8	5.8	11.8
11		2.1	16.5	1.7	14.8	48.8
12		3.4	26.2	2.3	23.9	102.0
13	10%	0.7	7.8	0.5	7.3	1.6
14		2.1	18.1	0.8	17.3	8.4
15		3.4	29.3	1.1	28.2	24.4
16	5%	0.7	7.9	0.1	7.8	0.6
17		2.1	19.3	0.3	19.0	2.5
18		3.4	30.3	0.6	29.7	8.4
19	2.5%	0.7	8.3	0.0	8.3	0.3
20		2.1	19.5	0.2	19.3	2.0
21		3.4	31.2	0.3	30.9	5.5
22	0%	0.7	8.3	0.0	8.3	0.0
23		2.1	19.7	0.0	19.7	0.0
24		3.4	30.0	0.0	29.9	0.0

Table 2: Model Coefficients and Statistics

<i>Parameter</i>	<i>Value</i>
a	2.564
b	5.766
c	4.869
d	1.337
SSE	865
SV	80611
R ²	98.93%

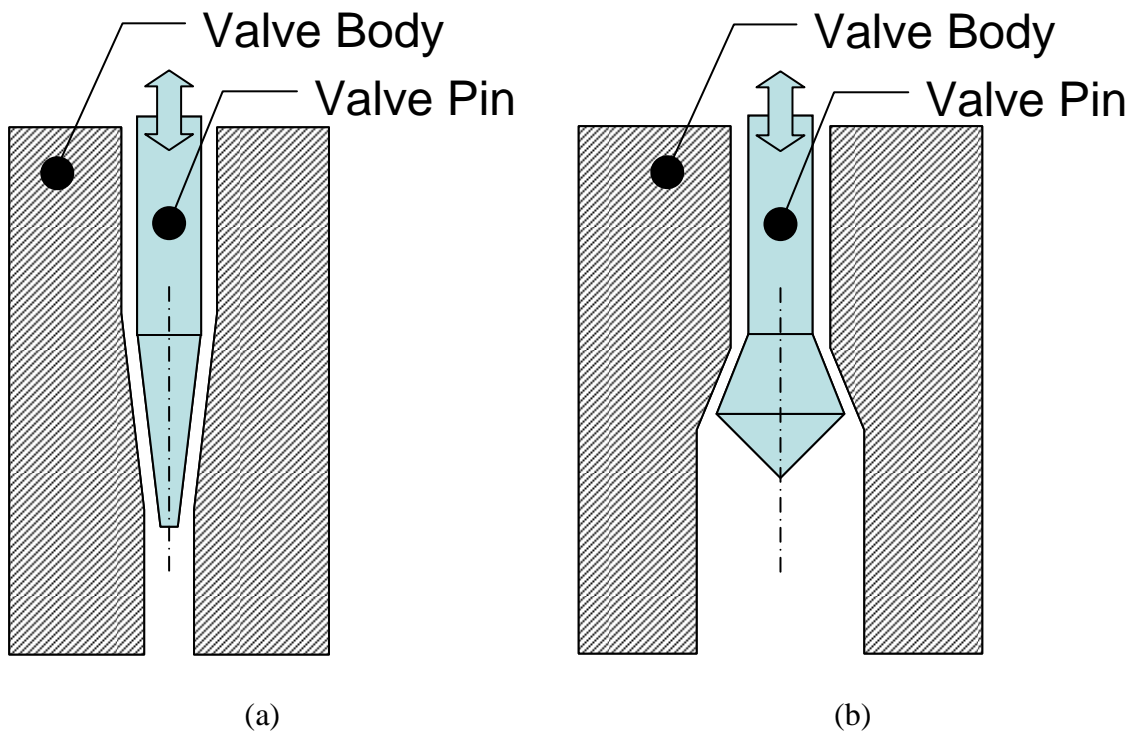


Fig. 1: Valve designs showing valve designs with (a) a forward taper, and
(b) a reverse taper

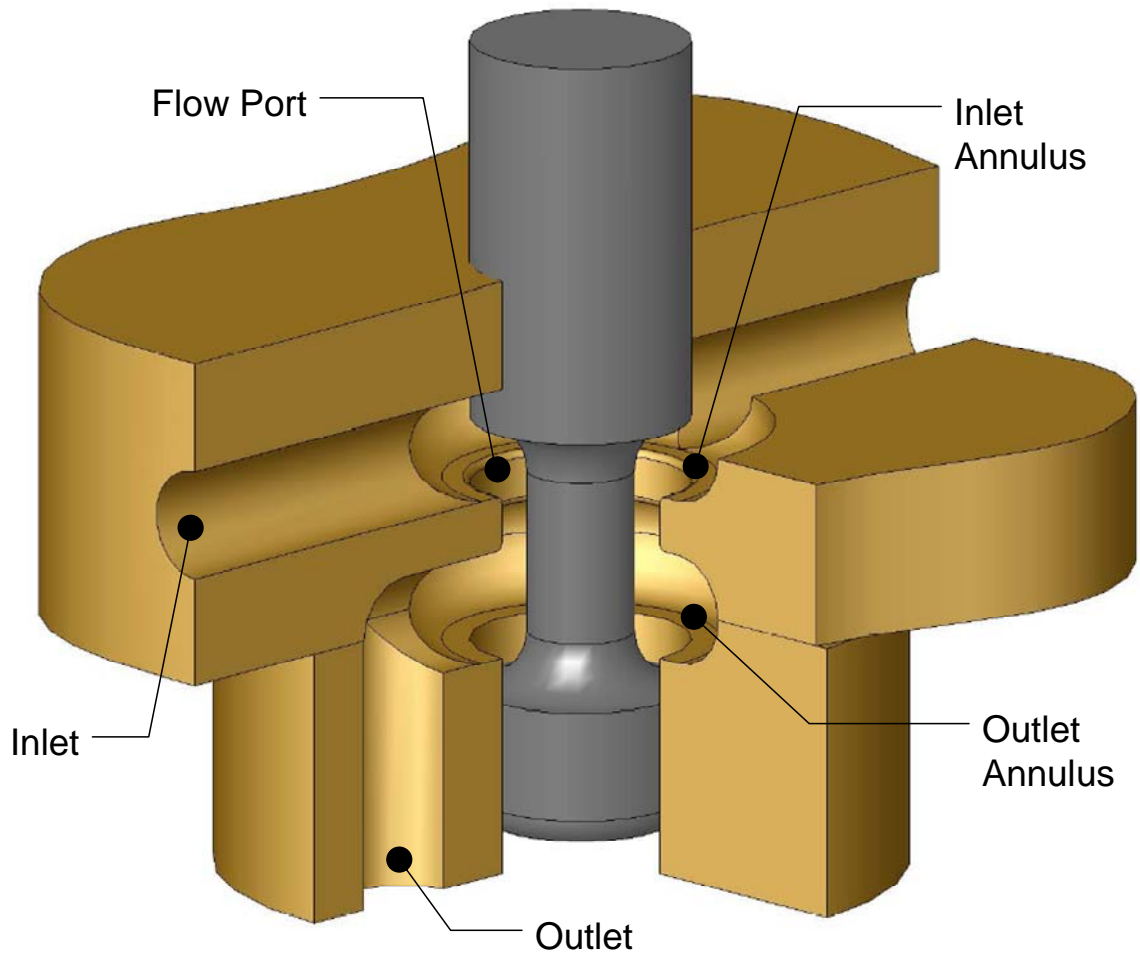


Fig. 2: Sectioned view of the axial valve design

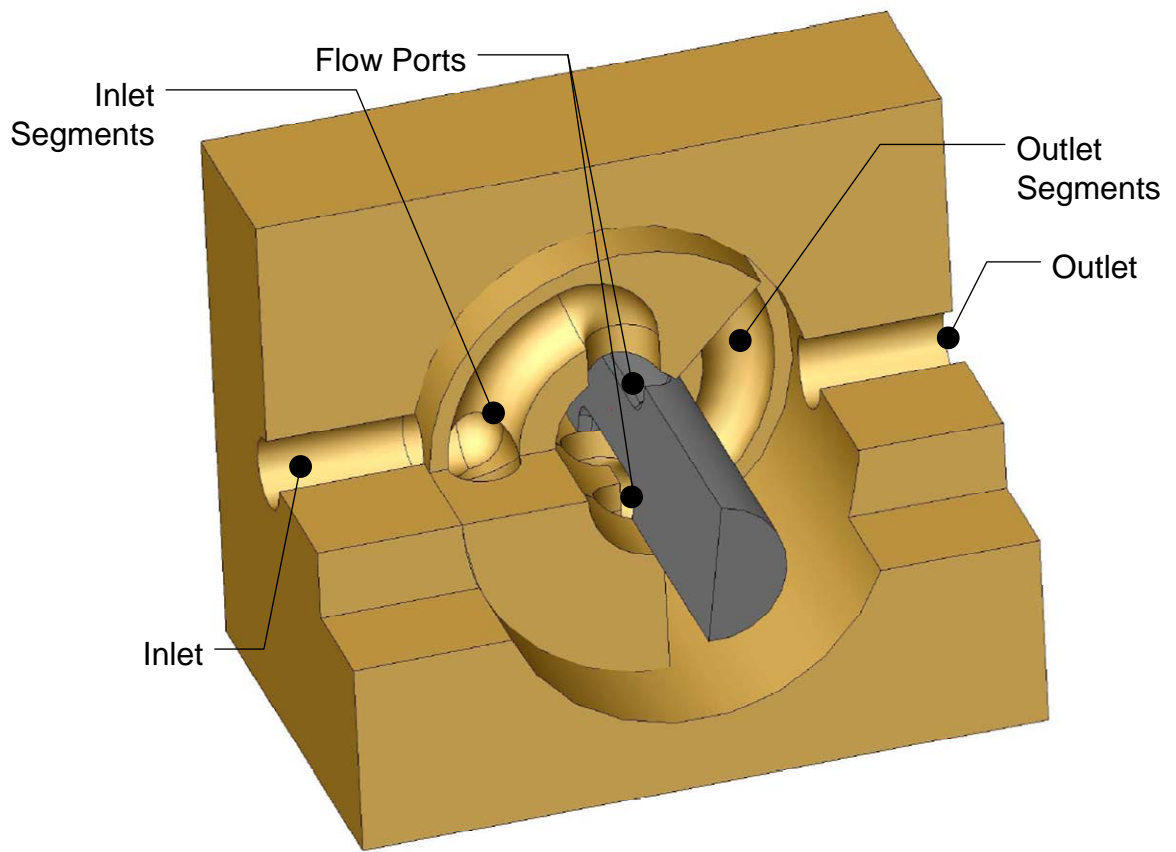


Fig. 3: Sectioned view of the rotary valve design

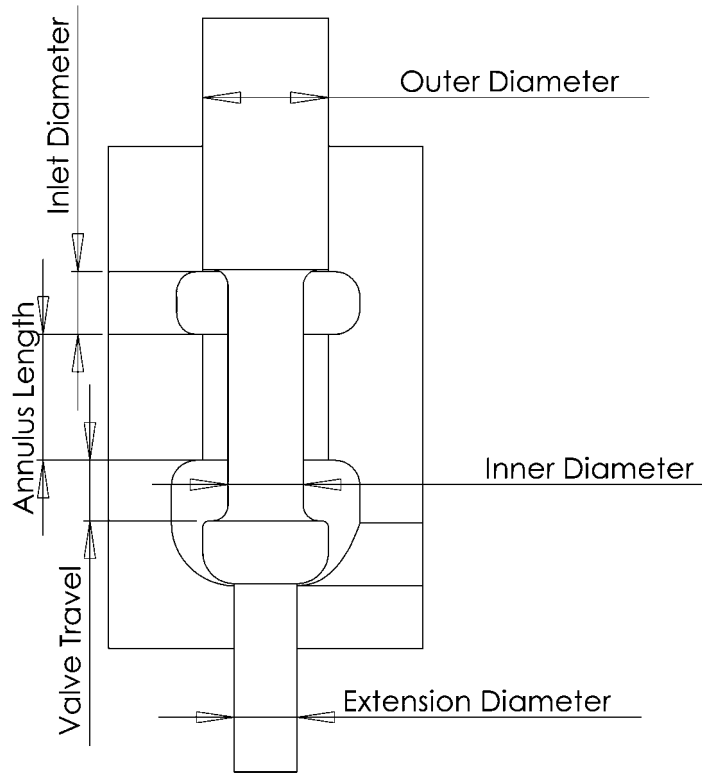


Fig. 4: Axial valve design parameters

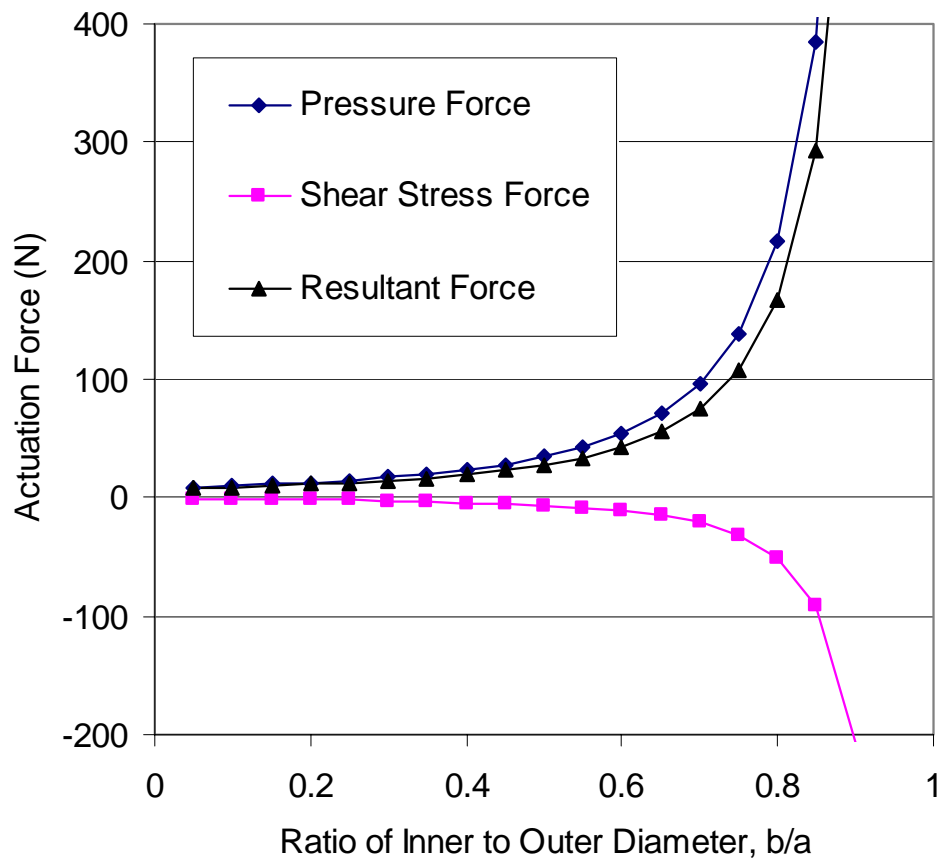


Fig. 5: Actuation forces as a function of ratio of inner to outer diameter, b/a

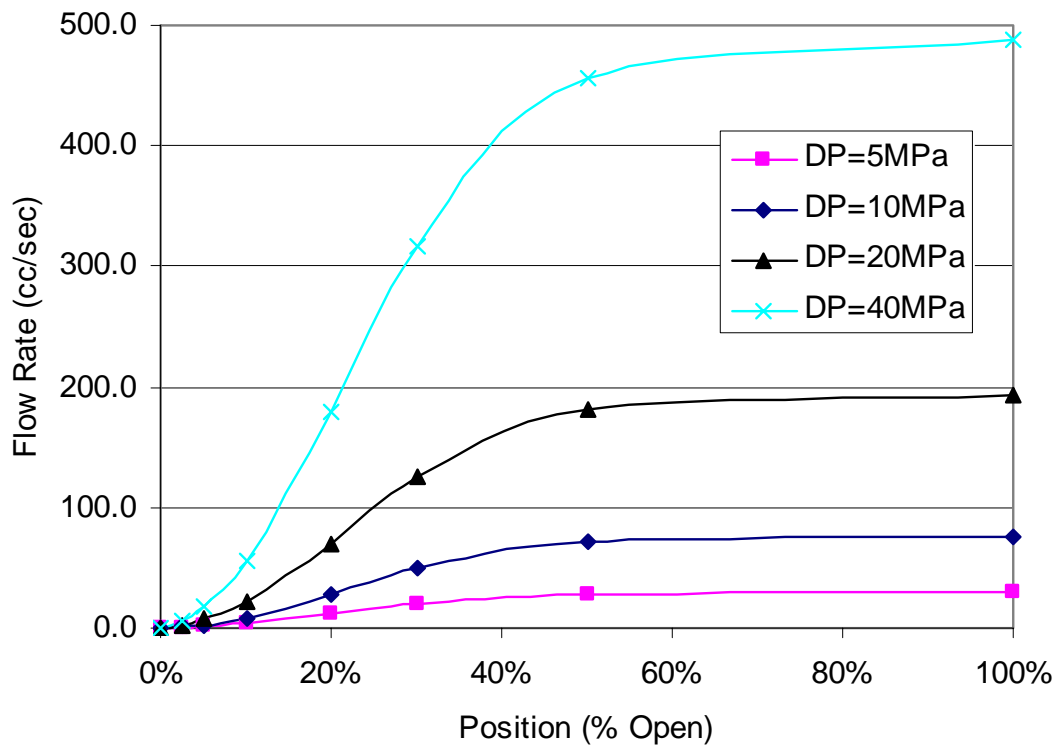


Fig. 6: Flow rate as a function of radial valve pin position

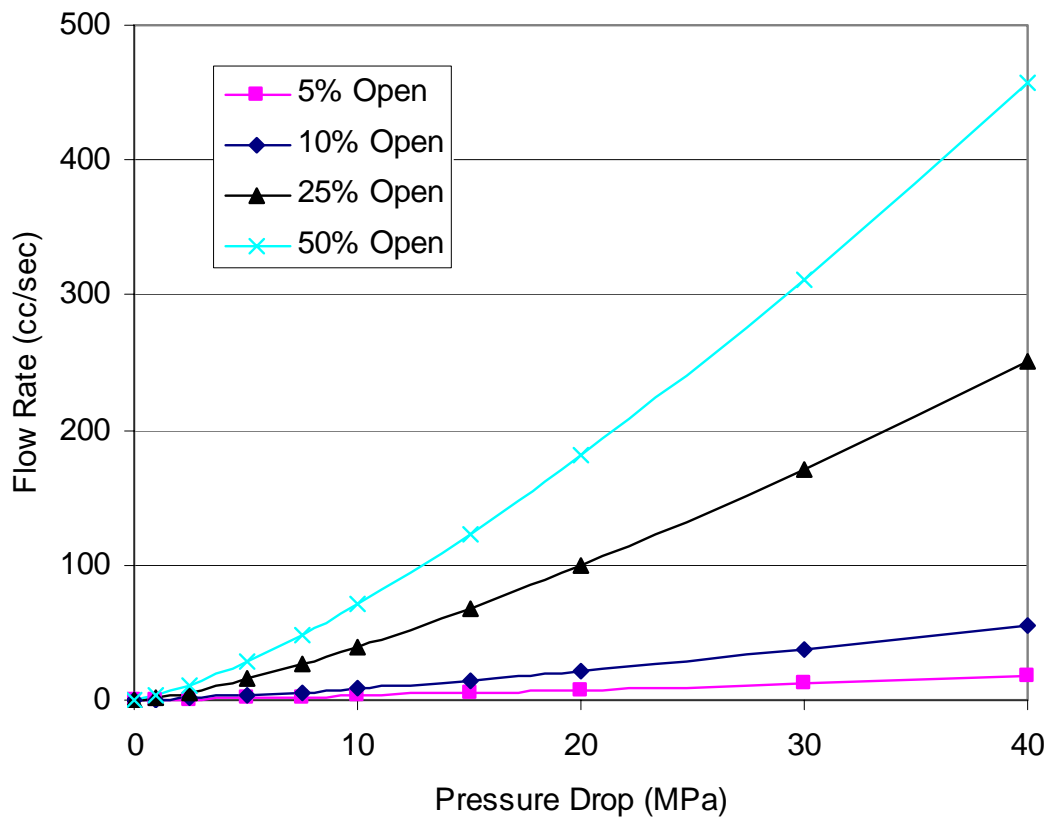


Fig. 7: Flow rate as a function of pressure drop

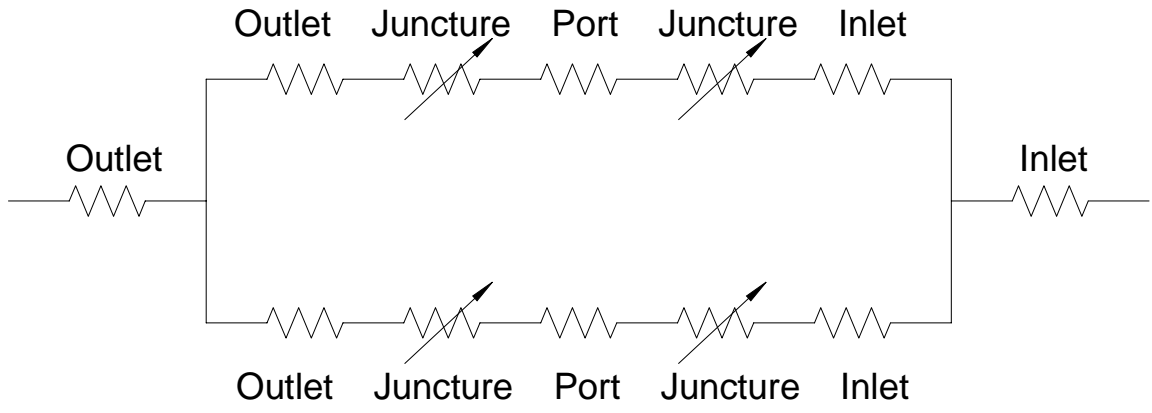


Fig. 8: Equivalent circuit model of flow through low force valve

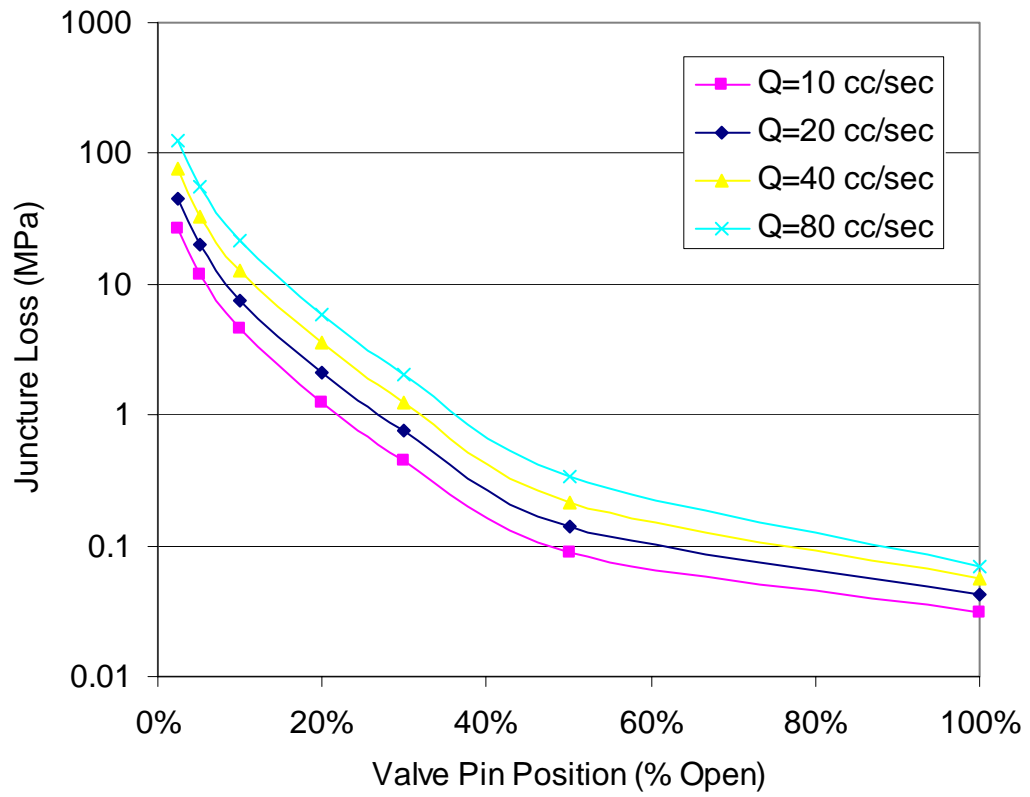


Fig. 9: Estimated juncture loss as a function of pin position and flow rate

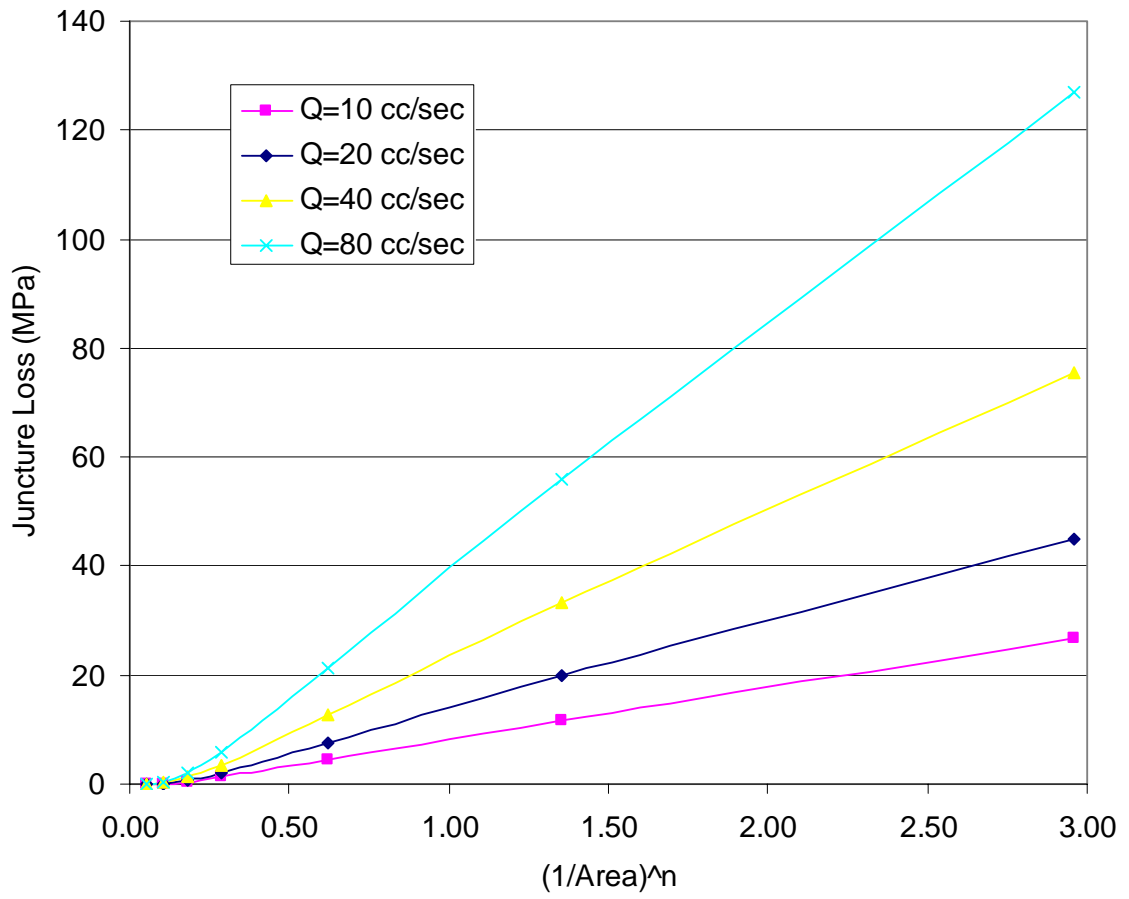


Fig. 10: Estimated juncture loss as a function of exposed area and power law index

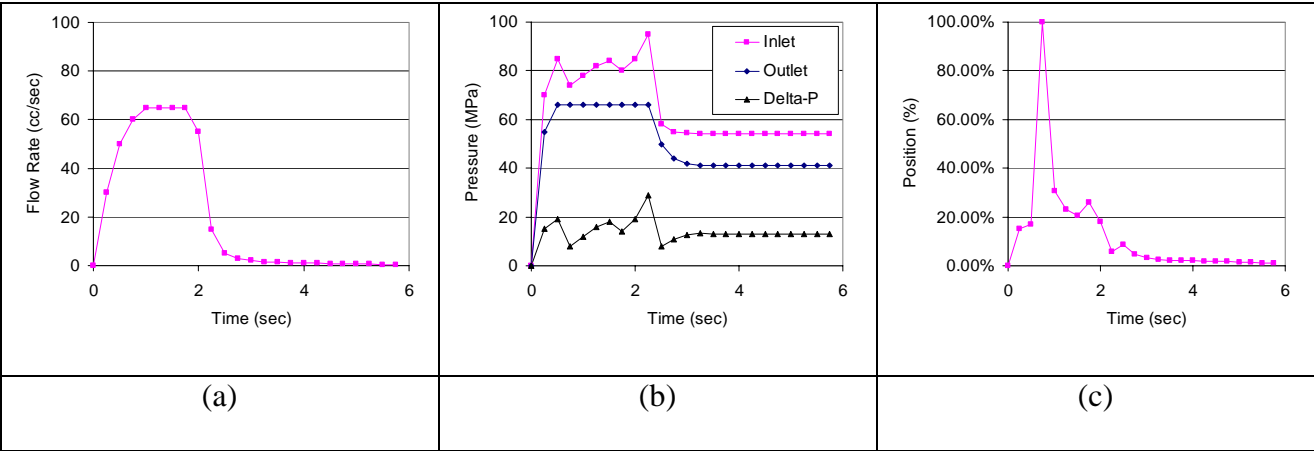


Fig. 11: (a) Flow rates, (b) pressures, and (c) pin position in a molding cycle

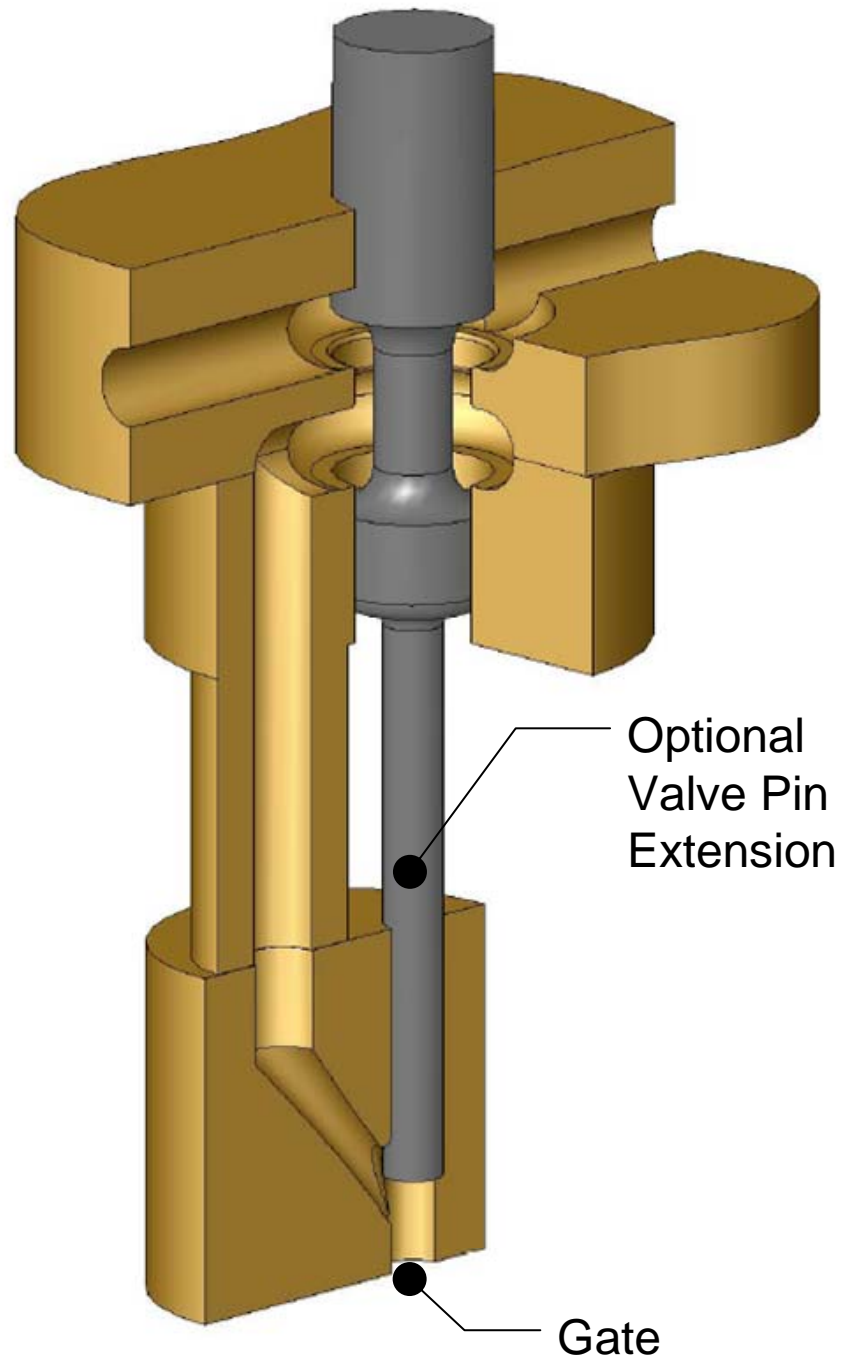


Fig. 12: Axial valve design with optional valve pin extension